MARS
The International Journal of Mars Science and Exploration

MARS INFORMATICS
Open Access Journals

Science and Technology

Integrating GPR and CCRI techniques: Implications for the identification and mapping of ground ice on Mars

Pablo A. Wainstein[1], Jean-Michel Wan Bun Tseung[1], Brian J. Moorman[1, 2], Christopher W. Stevens[1]

[1]*Department of Geography, University of Calgary, Calgary, Alberta, Canada, pawainst@ucalgary.ca;* [2]*Department of Geology and Geophysics, University of Calgary, Calgary, Alberta, Canada*

Citation: Mars 4, 1-13, 2008; doi:10.1555/mars.2008.0001
History: Submitted: April 23, 2007; Reviewed: July 2, 2007; Revised: October 3, 2007; Reviewed: November 23, 2007; Revised: January 10, 2008; Accepted: January 31, 2008; Published: April 14, 2008
Editor: Jeffrey B. Plescia, Johns Hopkins University
Reviewers: John A. Grant III, Smithsonian Institution; Robert E. Grimm, Southwest Research Institute

Abstract

Background: Since the early flyby missions of the 1970s, the study of Mars has largely focused on understanding the role of water (liquid or solid) in the geological evolution of the planet as well as its potential to support biotic activity. Data generated by the Mars Odyssey neutron and gamma ray spectrometers indicate large reservoirs of hydrogen (possibly H_2O ice) in the near surface of Mars at latitudes greater than 50°. Additionally, Viking Orbiters and the Mars Orbiter Camera have revealed numerous landforms, possibly related to ground ice and permafrost processes (*e.g.*, polygonal terrain, pingo-like mounds, thermokarst depressions, debris-aprons, and rock glacier-like features). However, despite observational evidence, an accurate identification and mapping of near-surface ground ice remains an open research question. Recently, the use of geophysical methods for investigating the Martian subsurface has witnessed growing interest among planetary scientists. Research involving the design and testing of geophysical instruments has focused primarily on Ground Penetrating Radar (GPR) and, to a lesser extent, seismic sounding, Time Domain Electromagnetic and Surface Nuclear Magnetic Resonance sounding.

Approach: The purpose of this study is to investigate the occurrence of ground ice in an area analogous to what may be found on Mars, the ice cored terrain surrounding Athabasca Glacier, Alberta, Canada; and to examine the combined applicability of two geophysical methods such as GPR and Capacitively Coupled Resistivity Imaging (CCRI) in the investigation of the ice-rich Martian environment.

Results and Implications: Our results show that GPR and CCRI techniques effectively complement each other by resolving different characteristics of the subsurface. While GPR clearly showed the subsurface structures and interfaces, CCRI provided diagnostic information about the subsurface lithologies. The two main implications of this combined application for the exploration Mars are: (a) it improves the ability to identify and map Martian ground ice; and, (b) it produces a more accurate description of the subsurface properties.

Introduction

The study of Mars has relied on many paths of research including the study of terrestrial analogues and the development of new and more powerful remote sensing instruments. However, this expansion in technology has focused primarily on the study of the Martian surface features and characteristics. With an increasing interest in Mars as a potential cradle for past or even contemporary biotic activity, the study of water in all its forms and probable locations has been at the top of the agenda of various research institutions including the National Aeronautics and Space Administration and their now famous missions' theme "follow the water." This is demonstrated by the recently launched Phoenix mission whose objectives are

to study the hydrologic history of the Martian arctic, to investigate the ice-soil boundary in order to assess the potential for biotic activity and to look for clues of a habitable zone. As a result the use of geophysical methods for investigating the Martian subsurface has witnessed growing interest among planetary scientists.

One of the keys to future exploration of Mars is the discovery of ground ice. While ground ice is common to Arctic and Antarctic regions of Earth, its presence on Mars would have several implications such as providing clues on past climatic conditions, indications on past or present biotic activity and an understanding of the hydrologic regime of the planet, past or present.

Debate concerning the presence of ground ice on Mars is not recent. Early indicators such as fluidized ejecta, inferred to be the consequence of the melting or vaporisation of ground ice and ground water caused by the impact (*e.g.*, Carr et al. 1977; Johansen 1979; Wohletz and Sheridan 1983; Battistini 1984; Horner and Greeley 1987; Barlow and Bradley 1990; Cave 1993; Costard and Kargel 1995), have been followed by thermal models which predict near-surface ground ice (*e.g.*, Farmer and Doms 1979).

The geomorphology of Mars suggests that it has gone through periods when the presence of liquid water was important in shaping the Martian surface, thus indicating conditions warm enough to sustain liquid water on the surface. However, the presence of other numerous landforms possibly related to ground ice and permafrost processes suggest that these conditions have changed over time, leading to a hydrologic system that resembles more that of permafrost regions. While the form of ground ice in the Martian crust is unknown, several geomorphic indicators suggest that it may be in the form of massive ground ice. Such features include thermokarst depressions (Costard and Kargel 1995; Soare et al. 2005, Wan Bun Tseung and Soare 2006) and pingo-like mounds (Burr 2005; Soare et al. 2005). Additionally, early indicators in the form of fluidized ejecta have been followed by thermal models, which suggest that ground ice exists or may have existed in the near surface (*e.g.*, Farmer and Doms 1979). In the case of fluidised ejecta, the ejecta mobility ratio of some rampart craters as described by Costard and Kargel (1995) could indicate the presence of large ice lenses in the ground and possibly massive ground ice. Furthermore, data generated by the Mars Odyssey neutron and gamma ray spectrometers indicate large reservoirs of hydrogen (possibly H_2O ice) in the near surface of Mars at latitudes greater than 50° (Boynton et al. 2002; Mitrofanov et al. 2002; Feldman 2004). Nevertheless, despite an extensive list of observational evidence, an accurate identification and mapping of near-surface ground ice remains a challenge.

This paper proposes a new technique that integrates two proven geophysical methods, Ground Penetrating Radar (GPR) and Capacitively Coupled Resistivity Imaging (CCRI) to effectively resolve subsurface structure and composition. Additionally, a discussion of the potential application of them in the identification and mapping of ground ice on Mars is presented.

Background: Geophysical techniques for the study of Mars

Research involving the design and testing of geophysical instruments for Mars has primarily focused on individual techniques including seismic sounding (*e.g.*, Nieto and Stewart 2003), Time Domain Electromagnetic (TDE) and Surface Nuclear Magnetic Resonance (SNMR) sounding (Grimm 2003) and GPR (*e.g.*, Grant and Schultz 1992; Oril and Ogliani 1996; Heggy et al. 2001; Arcone et al. 2002; Grant et al. 2003; Leuschen et al. 2003; Berthelier 2003). Recent analog studies using combined geophysical methods also involve multi-frequency GPR surveys (Stillman and Olhoeft 2006) combined with DC resistivity vertical electrical sounding and transient electromagnetic sounding (Clifford et al. 2006; Dinwiddie et al. 2006).

Today two space missions have been designed to use low-frequency ground penetrating radars. First, the Mars Advanced Radar Subsurface and Ionosphere Sounding (MARSIS) experiment on board the Mars Express Orbiter was launched in June 2003 and uses a high-gain antenna to sound from orbit (Picardi et al. 1999; Picardi et al. 2005). While MARSIS studies the surface-atmosphere interaction, it also uses its subsurface radar sounder to search for water to a depth of about 5 km. Second, launched in August 2005, the Shallow Subsurface Radar (SHARAD) on board the Mars Reconnaissance Orbiter has probed the Martian subsurface to a depth of about 1 km using a 20 MHz center frequency and 10 MHz bandwidths to complement the lower frequency (maximum frequency of 5 MHz) and bandwidth (1 MHz) capabilities of the MARSIS instrument (Seu et al. 2007). To date, geophysical surveys on Mars using MARSIS and SHARAD have primarily focused on the polar caps since the materials that make up these regions are most consistently amenable to subsurface sounding and include kilometre-thick water-ice-rich polar layered deposits (PLD), although some surveys were also conducted in the equatorial regions of Mars.

Initial results obtained from MARSIS over the north polar cap showed a strong reflection at a depth consistent with the elevation of the surrounding plains. This strong reflection suggests minimal electrical attenuation (consistent with a sediment-poor material) through about 2 km of polar deposits, indicating the presence of almost pure cold ice (<-24.15 C) (*e.g.*, Milkovich et al. 2007; Phillips et al. 2007; Plaut et al. 2007; Seu et al. 2007). Over both polar caps, MARSIS consistently has reached the base of the PLD, found at a maximum of 3 km depth at both poles.

Over the south polar cap of Mars, SHARAD primarily detected icy layered sediments (mostly water ice) overlain by a layer a few meters thick made of a carbon dioxide ice and dust mixture, protecting the water ice from decay (Seu et al., 2007). Other main subsurface features identified by SHARAD include: 1) layers within the South Polar Layered Deposits (SPLD); 2) reflections produced by the contact

between the SPLD and the underlying substrate located at 1.4 km depth (also observed by MARSIS) and 3) erosional unconformities (*e.g.*, Milkovich et al. 2007; Plaut et al. 2007; Putzig et al 2007; Seu et al. 2007). In southern Elysium Planitia, SHARAD detected radio-transparent deposits (up to 75 m thick) thought to be aqueous or sedimentary in origin. Similar deposits were also observed in Amazonis Planitia although SHARAD showed a reflector at ~40-90 m depth which is highly consistent with Earth-based radar backscatter at 12.6 cm wavelength, suggestive of lava flows (Safaeinili et al. 2007). Other future scout missions as well as the Astrobiology Field Laboratory could accommodate GPRs but are still at the planning level today.

According to Olhoeft (2001) resistivity represents one of the most appropriate methods to detect and quantify water in the Martian subsurface, since a change in the subsurface conductivity derived from the presence of water is effectively detected by resistivity techniques. Likewise, Stillman and Olhoeft (2006) argue that the lack of liquid water and its associated low conductivity in the Martian subsurface results in a good GPR environment although radar attenuation could occur due to dielectric and magnetic losses of subsurface materials or temperature variations (Kauzmann 1942; Dunlop and Özdemir 1997). Theoretically, the presence of highly conductive materials could vary the survey depth of penetration due to high energy absorption and signal attenuation. Heggy et al. (2001) supported this view and argued that the iron oxide rich layers of the Martian subsurface will in fact attenuate the GPR signal propagation and therefore special considerations must be taken in order to have a successful GPR survey in Mars. Additionally they suggest that the presence of moisture gradients (due to geothermal activity) and highly magnetic basaltic material could interfere with the propagation of electromagnetic waves.

However, Van Dam (2002), based on a study of GPR behaviour in the presence of iron oxides using time domain reflectometry, thermogravimetry and magnetic measurements, argued that GPR signals are not significantly attenuated by the presence of iron oxides per se. Furthermore, Olhoeft (2001) states that electromagnetic methods such as GPR, with frequencies in the order of tens to hundreds of MHz, could penetrate to depths of tens of meters through the Martian subsurface.

The successful application of shallow geophysical techniques on the Martian subsurface heavily depends on the knowledge of the subsurface electromagnetic characteristics and how these will affect wave propagation. As such, further investigations are required to adapt terrestrial techniques to properly work under Martian conditions.

Study site

The Athabasca Glacier (Figure 1), located in Jasper National Park, Alberta is one of the main outlet glaciers of the Columbia Icefield and was first described by Stutfield and Collie in 1897. The glacier is roughly 1 km wide and its depth along the longitudinal centreline varies between 300 m near its head to 60 m close to the snout (Kite 1977; Luckman 1988; Vachon et al. 1996; Matsuoka et al. 2003). Since its last Neoglacial maximum, the Athabasca Glacier has retreated to a present length of about 3.5 km between the terminus and the lowest icefall (Matsuoka et al. 2003).

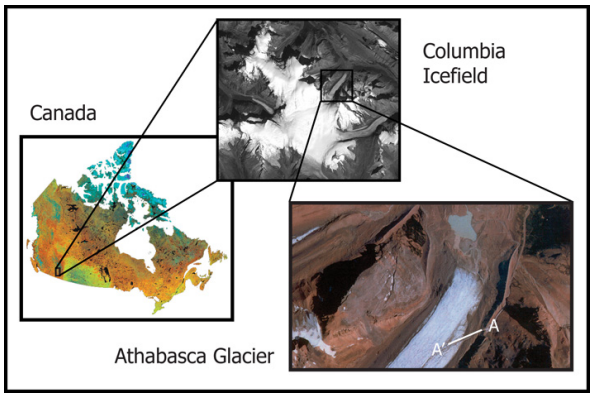

Figure 1. Study site. Line A-A' shows the snow coach access road where the surveys were conducted (figure1.jpg).

While the climatic conditions at the Athabasca Glacier are different from those existing on Mars, the geology and geomorphology of the area provide easy access to a variety of terrain not unlike those on Mars. These include proglacial till deposits, fine to coarse glacio-fluvial sediments, buried and exposed bedrock, bouldery surfaces, as well as terrain with different ice contents ranging from massive buried ice (ice-cored moraine and debris-covered glacier ice) to interstitial ice.

This study focuses on the moraine deposits on the south east side of the glacier. These moraine deposits are primarily composed of glacially transported debris comprising silt and clay-sized sediments mixed with gravelly material transported by the glacier. Loose, coarse, angular, non-striated clasts mainly sandstones produced by rock falls from the cliffs above the glacier also overly parts of the lateral moraine (Osborn 2006; Hart 2006).

An access road, where the moraine surface has been smoothed (Figure 2), runs from the proglacial area and along the east side of the southeast lateral moraine, accessing the glacier roughly 500 m up valley from the glacier's snout. For this study, surveys were conducted along the access road, having the contact zone between the glacier and the lateral moraine as the mid-point of the survey lines. An important aspect of these surveys is the presence of glacier ice beneath the access road along which GPR and CCRI transects were conducted. This buried ice results from moraine deposits falling onto the edge of the glacier. It is this combination of fine-grained sediments mixed with gravelly and bouldery material, underlain by massive ice that provides a good analogue for the testing of geophysical instruments for potential future Mars exploration.

Similar terrain types are thought to be extensive on Mars, including moraine like features in the Deuterolinus area (*e.g.*,

Head et al. 2005; Arfstrom and Hartmann 2005), fluvial deposits of the Circum-Chryse outflow channels (e.g., Lucchitta 1981; Lucchitta 1986; Carr 1996; Chapman and Kargel 1999) and Athabasca Valles (Burr 2005), the fluvio-lacustrine sediments of the Vastitas Borealis Formation (VBF) (e.g., Chapman 1994; McGill 2001; Tanaka et al. 2003) and bouldery surfaces of potential rock glaciers and protalus lobes in Candor Chasma (*e.g.*, Whalley and Azizi 2003). Each of these terrain types are thought to contain different water ice contents and buried ground ice similar to the area surrounding the Athabasca Glacier. While the ice chemistry on Mars remains unknown, geomorphological evidence including pingos (Soare et al. 2005; Burr et al. 2005; Paige and Murray 2006), thermokarst depressions and polygon pits (*e.g.*, Sharp 1973b; Anderson et al. 1973; Gatto and Anderson 1975; Theilig and Greeley 1979; Costard and Kargel 1995; Costard and Baker 2001; Seibert and Kargel 2001; Chapman et al. 2003; Mangold 2003; Wan Bun Tseung et al. 2006) suggest that the ice could be in the form of massive ice.

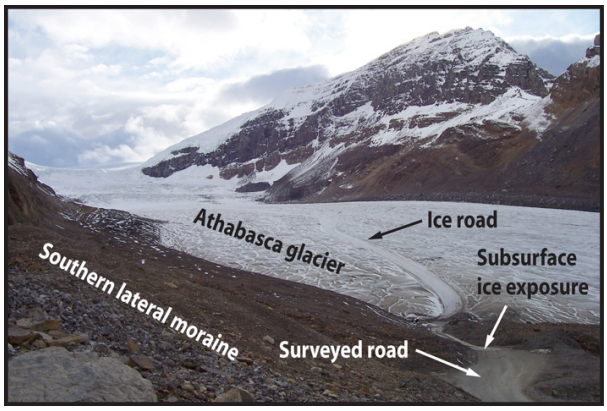

Figure 2. View of Athabasca glacier from its southern lateral moraine (figure2.jpg). The road in the foreground is 5 m wide.

Instruments

Ground Penetrating Radar

High fidelity digital GPR systems (Figure 3) became commercially available in the mid 1980s and by the mid-1990s were widely utilized for sedimentologic, glaciologic and ground ice investigations (Davis and Annan 1976; Annan 2002; Woodward and Burke 2007). It is a non-invasive geophysical technique capable of identifying changes in the shallow subsurface conditions through the generation and detection of reflected electromagnetic energy from electrically contrasting materials (Annan 2002; Neal 2004; Woodward and Burke 2007).

Ground penetrating radar systems are typically composed of a transmitter, a receiver, a pair of antennas, a controlling console, a computer and a power unit. The transmitter emits a short electromagnetic (EM) pulse that propagates into the subsurface. As the EM wave front travels through the ground, the energy is reflected, absorbed and/or scattered as a result of changes in the subsurface electromagnetic properties due to variations in porosity, lithology or water/ice content. By relocating the GPR system to different positions along a chosen survey line and recording the returns from further EM pulses, a profile of the subsurface is produced.

The response of GPR relies greatly on the ability of an interface to reflect a measurable amount of EM energy, expressed by the reflection coefficient (RC):

$$RC = \frac{\sqrt{\varepsilon_2} - \sqrt{\varepsilon_1}}{\sqrt{\varepsilon_2} + \sqrt{\varepsilon_1}} \quad (1)$$

where ε_1 stands for the dielectric constant in the upper medium and ε_2 the dielectric constant in the lower medium.

The RC ranges from 0 (no contrast in dielectric properties of different materials) to a maximum of about ± 0.8 (equivalent to a water-air boundary). As a result, GPR will display stronger reflections at boundaries separating units with highly contrasting dielectric properties. However, the RC scale is relative and therefore provides no direct information on the nature of the material surveyed.

The amplitude of a reflection depends on the difference between the dielectric constant (ratio between the material's electric static permittivity and the permittivity of vacuum) of two materials encountered (*e.g.*, ice: κ = 3-4, water: κ = 80, sediment: κ = 5-40, air: κ = 1). The material's dielectric properties vary mainly according to the character of the substance, its density and its water content. In contrast, the depth of signal penetration depends on the material's conductivity, the number and magnitude of reflections, the unit's power and the antennas' frequency (Moorman et al. 2003).

The ability of GPR to identify interfaces (sediment, ice, water or thermal) or point source reflections and produce an accurate image of the primary structures depends on the antenna frequency used and the step size of the survey. Ground penetrating radar antenna frequencies generally vary from 12.5 MHz to 1000 MHz, although the most commonly used center frequencies include; 50, 100 and 250 MHz. Lower frequencies are characterised by greater penetration depths but coarser resolutions, while higher frequencies typically exhibit low penetrations depths but higher resolutions. As a result, a trade-off between the depth of penetration and resolution exists (Davis and Annan 1989).

The high dielectric contrast between frozen and unfrozen materials and the low attenuation presented by ice makes GPR an effective tool for mapping areas of varying amounts of liquid and frozen water. As such, GPR has being successfully used, since the mid-1970s, in the detection of massive ground ice for scientific and engineering purposes (Kovacs and Morey 1985; Dallimore and Davis 1987; Robinson et al. 1993; Woodward and Burke 2007).

Figure 3. Noggin Plus 250 MHz ground penetrating radar system being pushed while conducting the survey on the access road located on the southern lateral moraine (figure3.jpg).

Capacitively Coupled Resistivity Imaging

Capacitively Coupled Resistivity Imaging (CCRI) (Figure 4) is a relatively new technique that emerged in the early 1990s, that provides a new and faster mode of survey in comparison to traditional direct current (DC) resistivity soundings. Unlike conventional electrodes planted in the ground, CCRI systems consist of a transmitter and a set of receivers with dipole antennas strung in array along a single cable which is pulled along the ground either by a person or by a vehicle.

The transmitter capacitively establishes an electrical field within the ground. The electrical field travels through the medium and the drop in voltage produced by its flow through the conducting ground is measured by the receivers.

One of the main advantages of CCRI is the ability to conduct surveys in areas where electrodes of traditional sting resistivity units would be difficult to implant into the ground such as permafrost, ice and bedrock. Additionally, the towing of the CCRI unit results in higher data acquisition rates.

The depth of penetration is mainly controlled by the electrode spacing, which can be varied according to the user's survey design. However, as a consequence of establishing the electrical field and not transmitting DC current directly into the subsurface, CCRI surveys tends to present shallower depth of investigations (5 to 10 m). Furthermore, the depth of penetration also depends on the resistivity of the subsurface material and its properties such as temperature, presence of water and texture of sediments (Reynolds 1997).

By interpreting the resistivity values of the various subsurface lithologies encountered, it is possible to determine the nature and composition of the subsurface.

Methodology

Ground penetrating radar and CCRI surveys were conducted on the access road (Figure 2) located on southern lateral moraine of Athabasca Glacier. A survey line, roughly 200 m long was established along the road. Survey flags were planted every 25 m as fixed reference points.

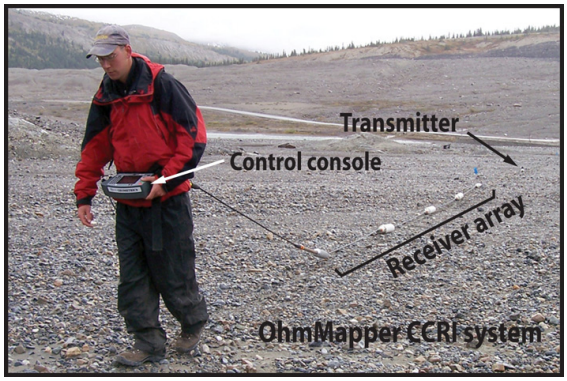

Figure 4. OhmMapper CCRI system being towed while conducting a resistivity survey (figure4.jpg).

In order to optimize the ability to detect subsurface features, two GPR systems were used:

1. PulseEKKO 100 (50 MHz and 100 MHz antenna frequencies) used in parallel broadside reflection mode with a constant separation between receiver and transmitter of 2 m and 1 m respectively, and a step size of 25 cm.

2. Noggin Plus (250 MHz antenna frequency) used in parallel broadside reflection mode with a step size of 5 cm and an antenna separation of 28 cm.

The profiles obtained with the Pulse Ekko 100 were generated with a 1000V transmitter and a stacking of 32, whereas the ones obtained with the Noggin Plus used a 100V transmitter and a stacking of 4. The processing of GPR profiles mainly included rubber banding to correct for small spatial inaccuracies, filtering of low frequency signal saturation (DEWOW) and the application of an Automatic Gain Control (AGC) to enhance lower amplitude returns. The processed profiles were then compared and selected according to their depth of penetration, resolution and ability to show the ice – debris interfaces at the foot of the moraine where glacier ice makes contact with the surrounding till.

The CCRI survey was conducted using an OhmMapper resistivity imaging system. In order to obtain the best resolution and depth of penetration, several two-way surveys were carried out over the same line with different array configurations. Four receivers were used with a 5 m dipole and a rope length between the first receiver and the transmitter of 10 m and 17.5 m for each run respectively. Under such a setup the survey achieved a maximum depth of penetration of 6 m.

Post processing of the raw CCRI data included the de-spiking of the profile to mute unrealistically high resistivity values considered as outliers, as well as the merging of the multiple pseudosections into one profile using Magmap (2000) software. The resistivity cross section was then calculated using the RES2D inversion package. The final inversion of the original pseudo sections was obtained after 5 iterations which brought down the Root Mean Squared (RMS) error to roughly 21%. This is considered a fairly good RMS error considering the highly heterogeneous subsurface and the large differences between resistivity values of the

debris and the glacial ice. As Bentley and Gharibi (2004) point out, 3D subsurface heterogeneities result in higher RMS errors in 2D inversions.

Merging of datasets

Ground penetrating radar and CCRI profiles were merged by following the subsequent steps:

First, each profile was topographically corrected and scaled based on elevation information supplied by a total station survey.

Second, in order to generate a depth scale for the GPR onto which the CCRI profile could be coupled, the propagation velocity of radar waves in the subsurface had to be determined. The velocity was calculated by migrating the profiles under increasing wave velocities and observing the collapse of hyperbolas until the optimal hyperbolic point source reflection collapse was achieved. Since the survey line includes several different materials and temperature conditions, the determination of single wave velocity was not feasible. Hence, the depth scales were calculated specifically to represent the material conditions of frozen till. The application of the above procedure gave a propagation velocity of 0.13 m ns^{-1}, which corresponds to the wave velocity for a frozen glacial till (Moorman et al. 2003). At this velocity the hyperbolas present in the ice were not collapsed giving an un-migrated look to the profile. However the profiles were migrated under the specific conditions that emphasized the area of interest (interface between frozen till and ice).

Finally, after the profiles had been scaled, topographically corrected and a depth scale was determined, they were graphically merged.

Resistivity forward modelling

Forward modelling was used to predict depth of penetration and resolution prior to the data collection and to study the effect that the thinning lateral margin of the glacier have on the resistivity profile. Using RES2DMOD software package, a block model of the ice-debris interface was created based on simplified structure taken from the GPR surveys and resistivity values of 5,000 ohm-m for till and 100,000 ohm-m for temperate glacial ice (Reynolds 1997).

The model was created following the same survey parameters as the actual CCRI field survey (Figure 5).

After the subsurface feature was modeled, the apparent resistivity pseudosection was calculated using RES2DMOD, which is then taken to RES2DINV to be inverted and thus the resistivity profile obtained.

Results

Resistivity forward modelling

The inversion of the resistivity model presents three main results (Figure 5). First, the modeled depth of penetration is

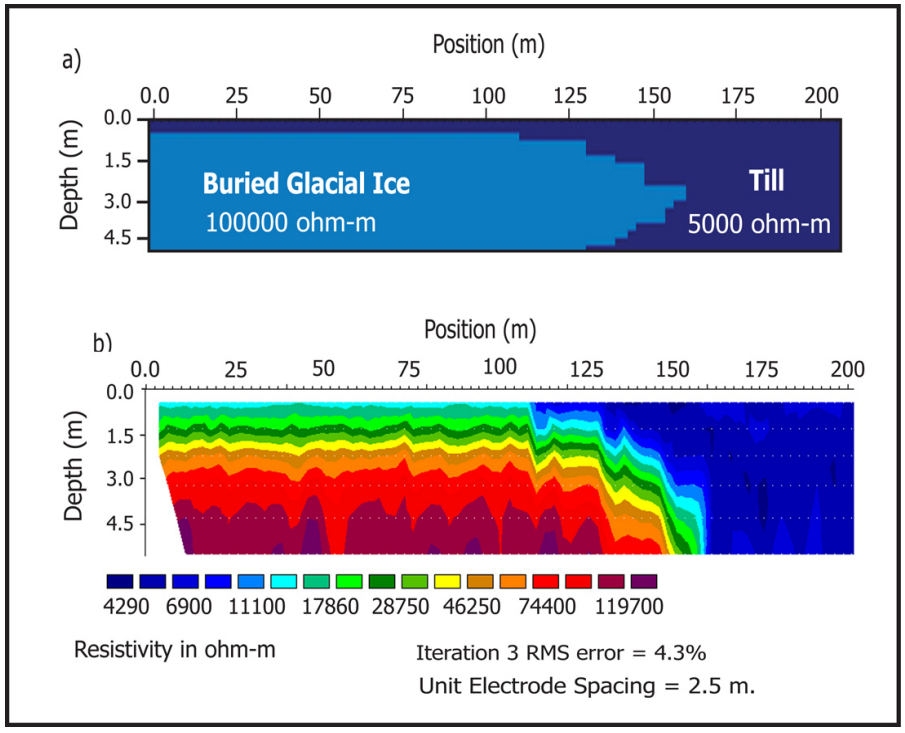

Figure 5. (a) Resistivity forward model of the lateral margin of the glacial ice and **(b)** inversion results of the resistivity model (figure5.jpg). Note that the sharp interface between till and glacial ice in the model is represented as a resistivity gradient in the inverted results.

approximate 5 metres. Second, the inverted profile presents an RMS error of 4.3% which is considerably lower than the one presented by the field survey as a result of the lack of heterogeneities in the modeled profile.

Third, gradational resistivity boundaries exist between the buried glacial ice and the surrounding till, showing that resistivity methods do not effectively delineate sharp interfaces. Therefore, an accurate delineation of subsurface interfaces, such as the one presented by the lateral margins of Athabasca Glacier, rely on the subjective interpretation of the person analyzing the data and/or on the comparison of the results with other complementary geophysical data sources or subsurface verification methods. These gradational resistivity boundaries are the result of the highly contrasting resistivity values between till and ice and the effect of this contrast in the interpolation process needed to obtain the contoured profile.

Interpretation of 50 MHz GPR profile

The GPR profiles obtained with 50 and 250 MHz antennas showed the least amount of noise, resulting in the best representation of the upper and lower (basal) ice-debris interfaces.

The 50 MHz GPR profile (Figure 6) can be divided into four main areas according to the reflection patterns or the lack thereof.

Near the beginning of the profile (A') there are two areas where reflections are noticeably different. Beneath the direct air and ground wave, the upper section shows a high density of hyperbolic reflections, which likely results from a significant concentration of shallow fractures in the ice and or englacial boulders. The lower section shows broader and weaker reflections thought to be the result of liquid water-rich glacial ice and adjacent subglacial sediments.

An area of highly attenuated signal begins at about 75 m and

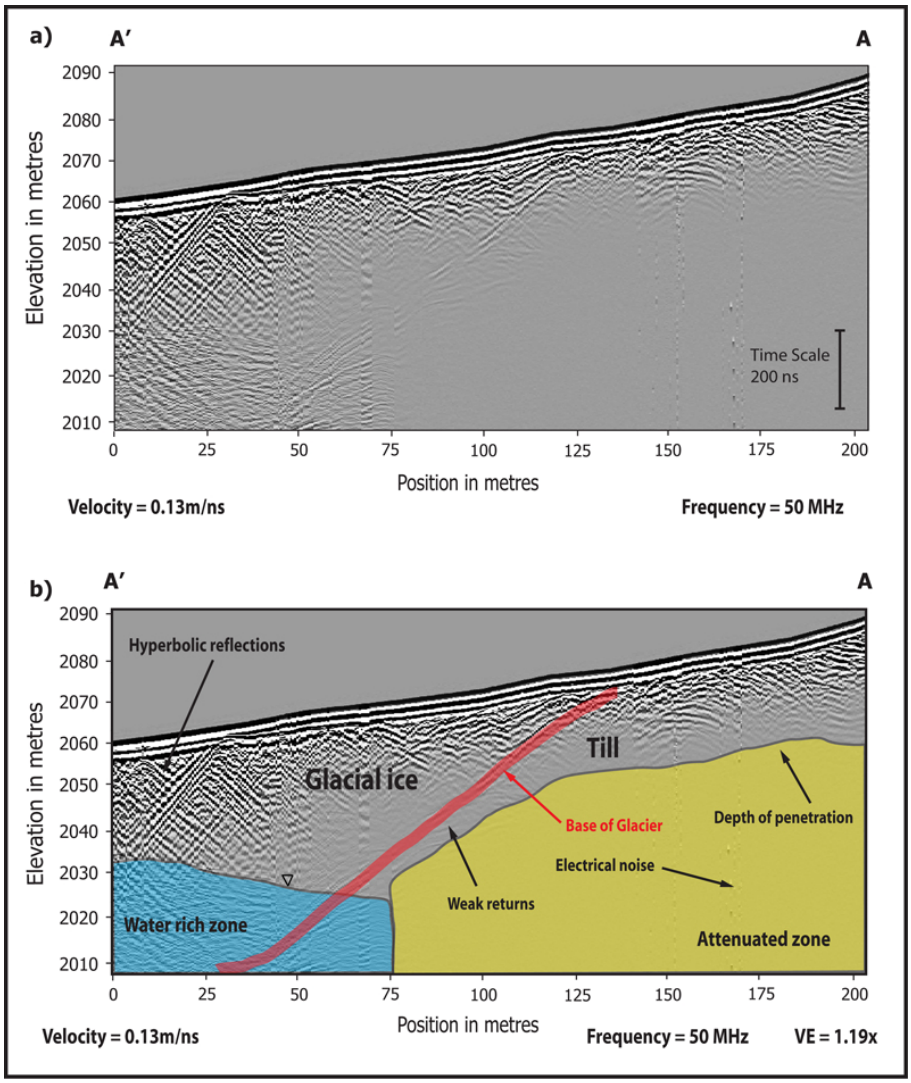

Figure 6. (a) Non-interpreted 50 MHz GPR profile and **(b)** interpreted 50 MHz GPR profile indicating the basal interface between glacial ice and till. Vertical exaggeration (VE) is 1.19x (figure6.jpg).

extends to 200 m along the profile, below depths of ~20 m. This probably results from a high concentration of conductive sediments (i.*e.*, clay minerals). As stated by Reynolds (1997), the conductivity of silts and clays with values as high as 0.25-0.05 S/m significantly attenuates the wave's energy, thus limiting signal penetration.

The profile also reveals a pronounced dipping reflection that extends from 25 to 135 m. Its migrated slope is ~28°. This continuous reflection has been interpreted as the lower (basal) interface between the glacier ice and the basal debris, based on its high reflection amplitude values.

Interpretation of the CCRI profile

Resistivity surveys resolved data to roughly 5.4 m. The CCRI profile (Figure 7) shows a high resistivity area that extends from 0 m up to 125 m along the profile.

Representative values for this area range from ~10,000 ohm-m to ~100,000 ohm-m which corresponds to the values of glacial temperate ice (Reynolds 1997). A second zone, of considerably lower values (~400 ohm-m to ~2,000 ohm-m) adjoins the high resistivity area interpreted as glacial till (Reynolds 1997). Additionally, there is a pocket of higher resistivity material, between 160 and 175 m, surrounded by a more conductive zone, which can be interpreted as an ice rich zone. The contact line between the high and the low resistivity zones (Figure 7) is characterised by a dipping front that extends from 90 m to 130 m with an average angle of 3°.

Interpretation of 250 MHz GPR profile

The 250 MHz profile (Figure 8a) presents a higher resolution image of the near subsurface. Using this antenna frequency, signal penetration was approximately 7 m, which closely matches the depth of penetration, achieved with the CCRI system. The profile shows three distinctive features. The most prominent feature is a high amplitude dipping reflection between the 110 and 160 m positions, with a migrated slope of 2.7°. This high amplitude reflection has been interpreted as the upper interface between the glacier ice and the debris cover (upper ice-debris interface) at the edge of the glacier.

Another feature of interest is a secondary reflection, or multiple, produced from the ice-debris interface. This multiple is located at roughly double the two-way travel time as the primary reflection and is the result of the large difference between the dielectric constants of ice and glacial till.

Located at the left side of the profile, there is vertical reflection patterns interpreted as spatially localized multiples generated in the near-surface ice fractures. When the radar wave encounters air filled ice fractures or crevasses reverberations between the fracture walls frequently produce this kind of reflection pattern. (Irvine-Fynn et al. 2006)

Data resolution: GPR versus CCRI

The CCRI's sensitivity analysis and spatial distribution of point measurements is shown in figure 9. The sensitivity value is a measure of the amount of resistivity information in each block of the inversion model. The higher the sensitivity

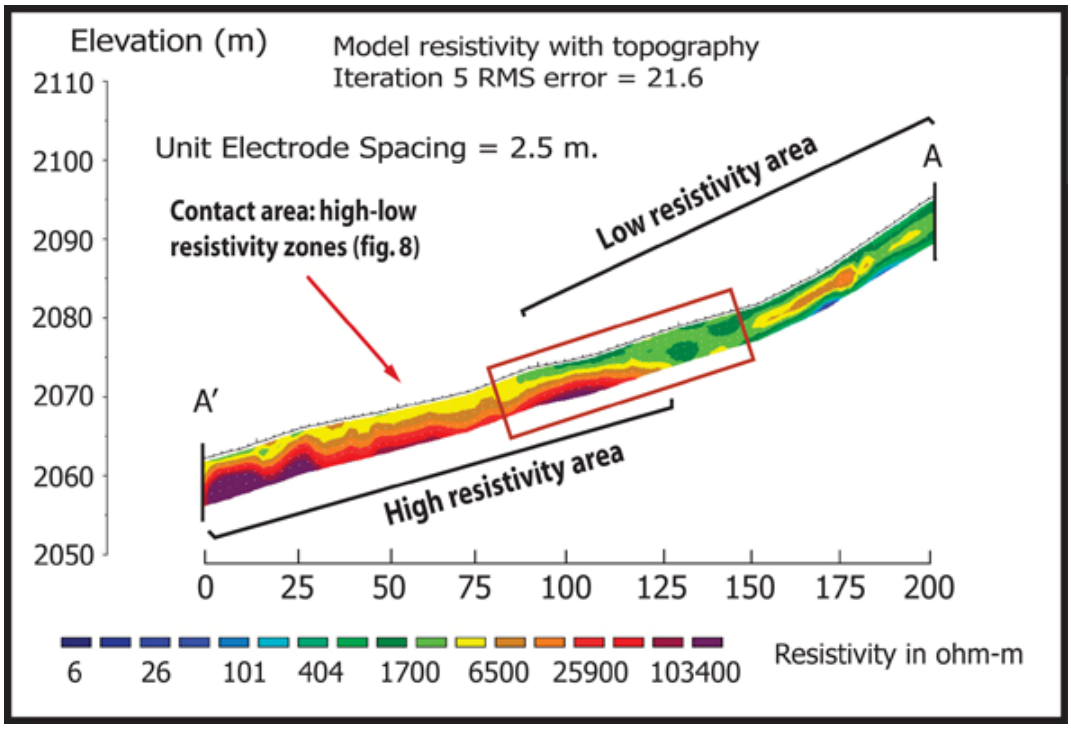

Figure 7. Resistivity survey profile showing a high resistivity area that extends from 0 m up to 125 m indicating the location of buried glacial ice. Note the pocket of higher resistivity material (160-175 m) which can be interpreted as an ice rich zone (figure7.jpg).

value, the more reliable is the fit between the inversion model and the measured data. The units are dimensionless and relational. They have been normalised by dividing them with the average sensitivity value. Based on the sensitivity analysis, it is suggested that the profile resolution varies between 2 to 20 metres, depending on the magnitude of the resistivity contrast. This results in gradual and smeared boundaries 5 m, or more, wide.

Ground penetrating radar, in contrast, presents a finer resolution and a higher capacity to resolve sharp boundaries. By definition, resolution is proportional to frequency (Neal 2004). Higher frequencies present a better ability to resolve objects than lower frequencies do. The 250 MHz profile presents a measured vertical resolution of approximate 20cm in frozen glacial sediments.

The horizontal area illuminated by the GPR electromagnetic waves, referred to as the radar footprint, depends on the antenna centre frequency, the depth of penetration (Neal 2004) and the material's dielectric constant. A 250 MHz survey with a depth of penetration of roughly 8 m would present an oval footprint with its long axis of about 5 m in frozen glacial sediments.

Analysis of merged data

The analysis of the merged profiles (Figure 8b) shows that the high amplitude dipping reflection revealed by the 250 MHz GPR profile correlates with the gradational boundary between the high and the low resistivity zones in the CCRI

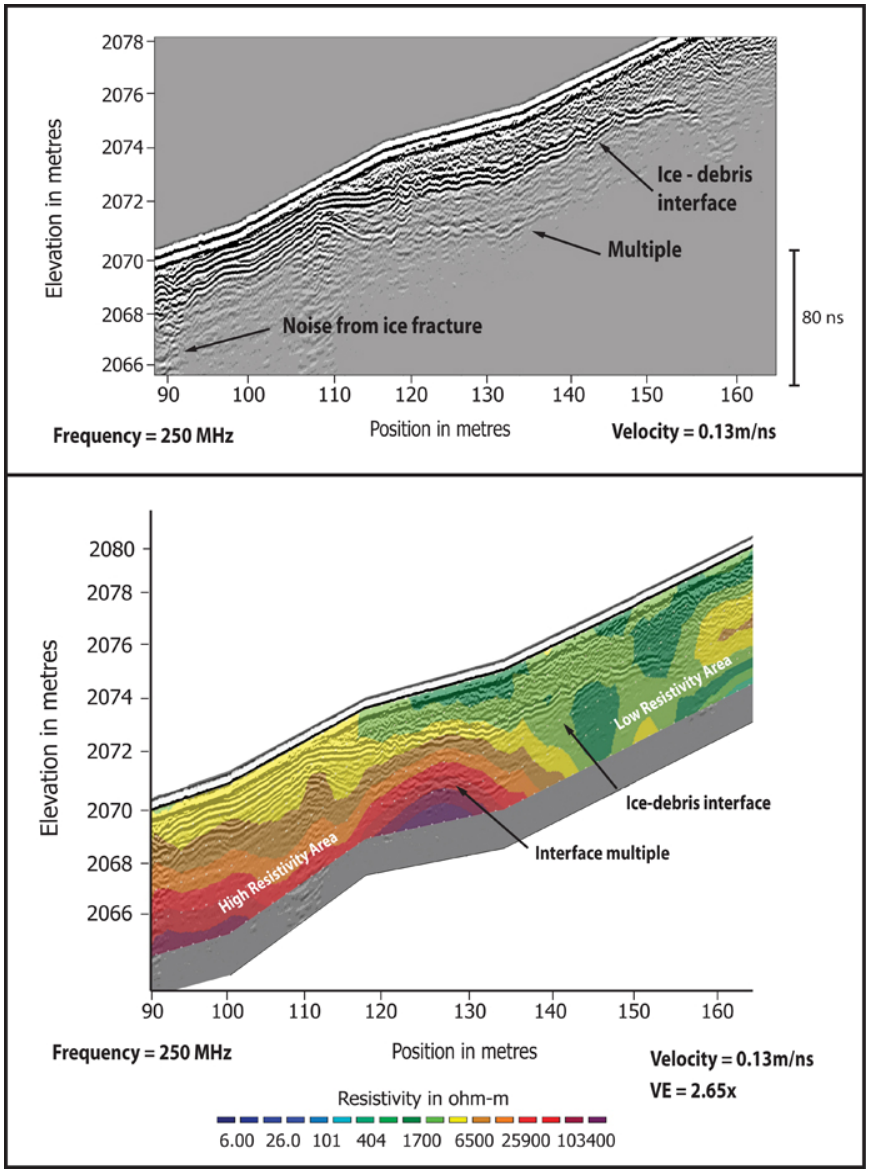

Figure 8. (a) 250 MHz GPR profile with topography correction and **(b)** 250 MHz GPR profile and CCRI profile merged together. Note the GPR resolves the upper interface between the glacial ice and the till, whereas the CCRI provides a material description. Vertical exaggeration (VE) is 2.65x (figure8.jpg).

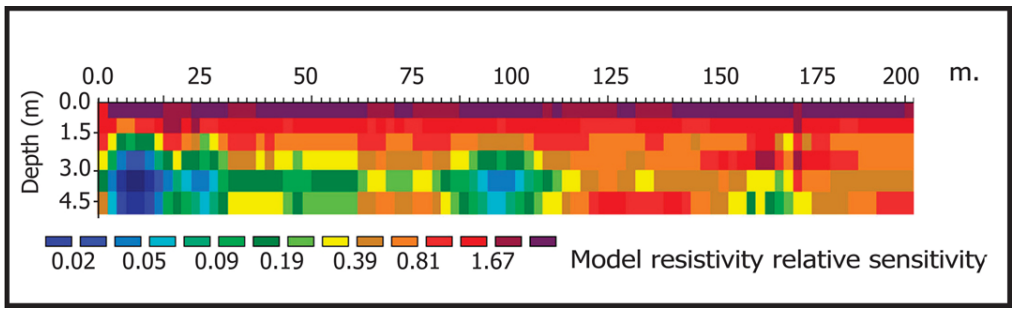

Figure 9. Sensitivity analysis of the CCRI profile. Areas with greater sensitivity have a larger impact on the quality of the fit between the inversion model and the measured resistivity data (figure9.jpg).

profile. However, the two cannot be spatially compared since the GPR shows a sharp well delineated interface whereas the CCRI presents a zone of transition. The width of this transition zone is attributed to the high resistivity contrast between ice and till.

The merging of the two data sets enabled a more complete interpretation of the subsurface (Figure 10), where each data source contributed to the interpretation by providing different types of data. The upper ice-debris interface is clearly shown by the 250 MHz GPR survey (Figure 8), whereas the lower (basal) ice-debris interface has been extracted from the 50 MHz profile (Figure 6).

Finally, the confirmation of the materials and their thermal state is given by the resistivity data obtained from the CCRI survey (Figure 7).

Discussion and Conclusions

The use of GPR for identifying and mapping subsurface features in terrestrial environments has proven successful. More specifically, the identification of ground ice in the southern lateral moraine of Athabasca Glacier was possible through the application of 50 MHz and 250 MHz GPR surveys. Their interpretation enabled the delineation of the buried glacier ice and its upper and lower (basal) debris-ice contact. However, it is notable that the identification of the materials on either side of such thermal and structural interfaces depends on the user's interpretation and understanding of the GPR system and the environment. As a result, subsurface verification methods such as borehole drilling, coring and excavations often accompany GPR investigations. For this study, subsurface verification of the geophysical data was accomplished through direct observation of the upper ice till contact line and at exposures to a depth up to 1.5 m near the edge of the glacier that ranged in size from 100 to 400 m^2.

On Mars, subsurface verification methods such as coring are not presently viable. Permafrost and coarse debris covered ground ice (*e.g.*, rock glaciers) have proven to be technically very difficult and costly to core even on Earth. The restrictions associated with travelling to Mars exacerbate this problem.

The resistivity profile obtained on the lateral moraine of Athabasca Glacier clearly shows the presence of a high resistivity body with values corresponding to ice, thus enabling a material identification of the feature delineated by the GPR profiles. Therefore, the combined use and integration of GPR and CCRI proved to be highly beneficial in a more objective interpretation of the subsurface of Athabasca's southern lateral moraine and especially in the identification and quantitative description of the ice-cored terrain.

Capacitively coupled resistivity imaging provides a powerful indirect method for subsurface verification of the GPR interpretation and the results obtained show that the application of both GPR and CCRI techniques together enables a considerably more confident and objective interpretation of the thermal and lithological structure of the subsurface, otherwise unobtainable except through extensive drilling.

Even though GPR and CCRI complement each other, there are some limitations to how accurate the merging can be. First, resistivity imaging is poor at spatially resolving sharp dipping interfaces such as the one presented by the glacier's thinning lateral margin (Figure 9). Additionally, the high

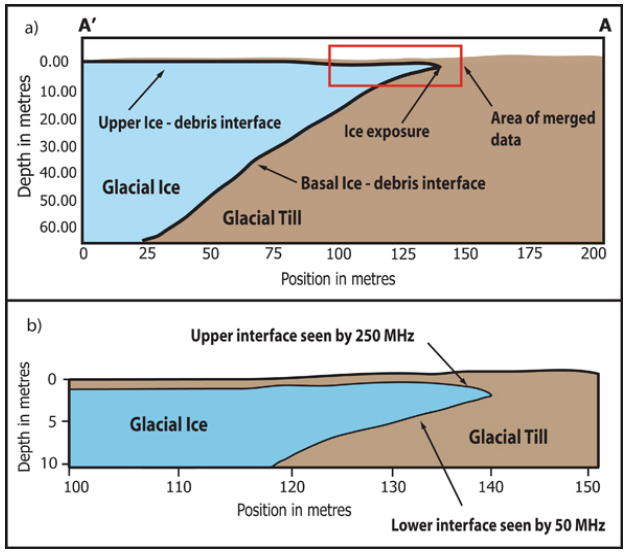

Figure 10. Schematic interpretation of the subsurface. Part (a) shows the complete survey line whereas (b) is a zoom in of the area where the GPR and CCRI profiles were merged (figure10.jpg).

resistivity contrast between the debris and the ice results in wide (5 m or more) gradational boundaries (Figure 8b). Second, the resolution of both methods does not correlate well to each other. While the 250 MHz GPR had a vertical resolution of less than 20 cm, CCRI had an effective resolution as great as 20 m.

The development of GPR and other geophysical techniques have considerably improved during the past two decades and are likely going to be an integral part of future Mars missions. The ability to identify and map near-surface massive ground ice as well as the possibility of quantifying ground ice volumes (hence water) using GPR and CCRI would prove beneficial to the continuing exploration of Mars, including the selection of future landing sites. Additionally, GPR and CCRI systems are portable and easy to operate on different types of surfaces when compared to other geophysical systems, such as DC resistivity or seismic sounding. The ability to conduct GPR and CCRI surveys without direct human interaction is certainly an added advantage for future exploration missions and will contribute to a better understanding of the Martian geology.

Directory of supporting data

root directory

manuscript.pdf this file

Fig. 1: figure1.jpg full-resolution image

Fig. 2: figure2.jpg full-resolution image

Fig. 3: figure3.jpg full-resolution image

Fig. 4: figure4.jpg full-resolution image

Fig. 5: figure5.jpg full-resolution image

Fig. 6: figure6.jpg full-resolution image

Fig. 7: figure7.jpg full-resolution image

Fig. 8: figure8.jpg full-resolution image

Fig. 9: figure9.jpg full-resolution image

Fig. 10: figure10.jpg full-resolution image

Acknowledgements

This research was supported by the University of Calgary GSA Research Project grant, and was carried out under Parks Canada research permit JNP-2006-763. We would like to express our thanks to Brewster Snow Coaches since they actively helped us with field support and logistics, as well as Chris Hugenholtz for assisting with fieldwork and review of this manuscript.

References

Anderson, D., L. W. Gatto and F. Ugolini (1973) "An examination of Mariner 6 and 7 imagery for evidence of permafrost terrain on Mars" Permafrost: Second International Conference (F. G. Sanger edition), 499-508. National Academy of Sciences, Washington, DC.

Annan, A. P. (2002) "GPR – history, trends and future developments" Subsurface Sensing Technologies and Applications 3, 4, 253-270. doi: 10.1023/A:1020657129590

Arcone, S. E., M. L. Prentice, A. J. Delaney (2002) "Stratigraphic profiling with ground-penetrating radar in permafrost. A review of possible analogs for Mars" Journal of Geophysical Research 107, E11, 5108. doi:10.1029/2002JE001906

Arfstrom, J. and W. K. Hartmann (2005) "Martian flow features, moraine-like ridges, and gullies: Terrestrial analogs and interrelationships" Icarus 174, 321-335. doi:10.1016/j.icarus.2004.05.026

Battistini, R. (1984) "L'utilisation des crateres meteoriques a ejectas fluidises comme moyen d'etude spatiele et chronologique de l'eau profonde (hydro lithosphere) de Mars" Revue geomorfologique et dynamique 33, 25-41.

Barlow, N. G. and T. L. Bradley (1990) "Martian impact craters: correlations of ejecta and interior morphologies with diameter, latitude and terrain" Icarus 87, 1, 156-179. doi:10.1016/0019-1035(90)90026-6

Bentley, L. R. and M. Gharibi (2004) "Two- and three-dimensional electrical resistivity imaging at a heterogeneous remediation site" Geophysics 69, 3, 674-680. doi: 10.1190/1.1759453

Berthelier, J. J. (2003) "GPR, a ground penetrating radar for the Netlander mission" Journal of Geophysical Research 108, E4, 8027. doi:10.1029/2002JE001866

Boynton, W. V. (2002) "Distribution of hydrogen in the near-surface of Mars: Evidence for subsurface ice deposits" Science 296, 81-85. doi:10.1126/science.1073722

Burr, D. M. (2005) "Clustered streamlined forms in Athabasca Valles, Mars: Evidence for sediment deposition during floodwater ponding" Geomorphology 69, 242-252. doi:10.1016/j.geomorph.2005.01.009

Burr, D. M., R. J. Soare, J.-M. Wan Bun Tseung and J. P. Emery (2005) "Young (late Amazonian), near-surface, ground ice features near the equator, Athabasca Valles, Mars" Icarus 178, 56-73. doi:10.1016/j.icarus.2005.04.012

Carr, M. H. (1996) Water on Mars, New York, Oxford University Press.

Carr, M. H., L. S. Crumpler, J. A. Cutts, R. Greeley, J. E. Guest and H. Masursky (1977) "Martian impact craters and emplacement of ejecta by surface flow" Journal of Geophysical Research 82, 4055-4065.

Cave, J. A. (1993) "Ice in the northern lowlands and southern highlands of Mars and its enrichment beneath the Elysium lavas" Journal of Geophysical Research 98, E6, 11079-11097.

Chapman, M. G. (1994) "Evidence, age and thickness of a frozen paleolake in Utopia Planitia, Mars" Icarus 109, 393-406. doi:10.1006/icar.1994.1102

Chapman, M. G. and J. S. Kargel (1999) "Observations at the Mars Pathfinder Site-Do they provide "unequivocal" evidence of catastrophic flooding?" Journal of Geophysical Research 104, 8671-8678.

Chapman, M. G., M. T. Gudmundsson, A. J. Russel and T. M. Hare (2003) "Possible Juventae Chasma subice volcanic eruptions and Maja Valles ice outbursts floods on Mars: Implication of Mars Global Surveyor crater densities, geomorphology, and topography" Journal of geophysical research, 108, E10, 5113. doi:10.1029/2002JE002009

Clifford, S. M. (2006) "Mars analog investigations of the West Egyptian desert utilising multi-frequency GPR and other electromagnetic sounding techniques" Lunar and Planetary Science Conference 37th, Abstract #2442.

Costard, F. and J. S. Kargel (1995) "Outwash plains and thermokarst on Mars" Icarus 114, 93-112. doi:10.1006/icar.1995.1046

Costard, F. M. and V. R. Baker (2001) "Thermokarst landforms and processes in Ares Valles, Mars" Geomorphology, 37, 289-301. doi:10.1016/S0169-555X(00)00088-X

Dallimore, S. R. and J. L. Davis (1987) "Ground-probing radar investigations of massive ground ice and near surface geology in continuous permafrost" Current Research, Part A, Geological Survey of Canada Paper 87-1A, 913-918.

Davis, J. L. and A. P. Annan (1976) "Impulse radar soundings in permafrost" Radio Science 11, 4, 383-394.

Davis, J. L. and A. P. Annan (1989) "Ground-penetrating radar for high-resolution mapping of soil and rock stratigraphy" Geophysical Prospecting 37, 5, 531-551. doi:10.1111/j.1365-2478.1989.tb02221.x

Dinwiddie, C. L., S. K. Sandberg, R. N. McGinnis and R. E. Grimm (2006) "Geophysical field investigation of a potential hyper-arid desert analog to Mars: The Western desert of Egypt" 37th Lunar and Planetary Science Conference, Abstract #2335.

Dunlop, D. J. and O. Özdemir (1997) "Rock Magnetism: fundamentals and frontiers" Cambridge University Press.

Farmer, C. B. and P. E. Doms (1979) "Global seasonal variations of water vapor on Mars and the implications of permafrost" Journal of Geophysical Research 84, 2881-2888.

Feldman, W. C. (2004) "Global distribution of near-surface hydrogen on Mars" Journal of Geophysical Research 109, E0, 9006. doi:10.1029/2003JE002160

Gatto, L. W. and D. M. Anderson (1975) "Alaskan thermokarst terrain and possible Martian analog" Science 188, 255-257. doi:10.1126/science.188.4185.255

Grant, J. A. and P. H. Schultz (1992) "Ground penetrating radar as a tool for investigating near-surface stratigraphy on Mars" Lunar and Planetary Institute Technical Report 92-07, Houston: 5-7.

Grant, J. A., A. E. Schutz and B. A. Campbell (2003) "Ground penetrating radar as a tool for probing the shallow subsurface of Mars" Journal of Geophysical Research 108, E4, 8024. doi:10.1029/2002JE001856

Grimm, R. E. (2003) "A comparison of time domain electromagnetic and surface nuclear magnetic resonance sounding for subsurface water on Mars" Journal of Geophysical Research 108, E4, 8037. doi:10.1029/2002JE001882

Hart, J.K. (2006) "Athabasca Glacier, Canada – a field example of subglacial ice and till erosion?" Earth Surface Processes and Landforms 31, 65-80. doi:10.1002/esp.1233

Head, J. W., D. R. Marchant and J. L. Fastook (2005) "Regional mid-latitude glaciation on Mars: Evidence for marginal glacial deposits adjacent to lineated valley fill" 36th Lunar and Planetary Science Conference, Abstract #1257.

Heggy, E., P. Paillou, G. Ruffie, J. M. Malezieux, F. Costard and G. Grandjean (2001) "On the water detection in the Martian subsurface using sounding radar" Icarus 154, 244-257. doi:10.1006/icar.2001.6717

Horner, V. M. and R. Greeley (1987) "Effects of elevation and ridged plains thicknesses on Martian crater ejecta morphology" Journal of Geophysical Research 92, B4, E561-E569.

Irvine-Fynn, T. D. L., B. J. Moorman, J. L. Williams and F. S. Walter (2006) "Seasonal changes in ground-penetrating radar signature observed at a polythermal glacier, Bylot Island, Canada" Earth Surface Processes and Landforms 31, 892-909. doi:10.1002/esp.1299

Johansen, L. A. (1979) "Martian splosh cratering and its relation to water" NASA Conference Publication 2072, 44.

Kauzmann W. (1942) "Dielectric relaxation as a chemical rate process" Review of Modern Physics 15, 12-44.

Kite, G. W. and I. A. Reid (1977) "Volumetric change of the Athabasca Glacier over the last 100 years" Journal of Hydrology 32, 279-294.

Kovacs, A. and R. M. Morey (1985) "Impulse radar sounding of frozen ground" In Workshop on Permafrost Geophysics, Golden, Colorado. US Army Corps of Engineers, Cold Regions Research and Engineering Laboratory, Hanover, New Hampshire, CRREL Special Report 85, 5, 28-40.

Leuschen, C., P. Kanagaratnam, K. Yoshikawa, S. Arcone and P. Gogineni (2003) "Design and field experiments of a ground penetrating radar for Mars exploration" Journal of Geophysical Research 108, E4, 8034. doi:10.1029/2002JE001876

Lucchitta, B. K. (1981) "Mars and Earth: Comparison of cold-climate features" Icarus 45, 264-303. doi:10.1016/0019-1035(81)90035-X

Lucchitta, B. K., H. M. Ferguson and C. Summers (1986) "Sedimentary deposits in the northern lowland plains, Mars" Journal of Geophysical Research, 91, B13, E166-E174.

Luckman, B. H. (1988) "Dating the moraines and recession of Athabasca and Dome Glaciers, Alberta, Canada" Arctic and Alpine Research 20, 1, 40-54.

Mangold, N. (2003) "Geomorphic analysis of lobate debris aprons on Mars at Mars Orbiter Camera scale: Evidence for ice sublimation initiated by fractures" Journal of Geophysical Research 108, E4, 8021. doi:10.1029/2002JE001885

Matsuoka, K., T. Aoki, T. Yamamoto and R. Naruse (2003) "Field performance tests of a portable low frequency ice penetrating radar and a ground penetrating radar at Athabasca Glacier, Canadian Rockies" Bulletin of Glaciological Research 20, 49-55.

McGill, G. E. (2001) "The Utopia Basin revisited: Regional slope and shorelines from MOLA profiles" Geophysical Research Letters 28, 411-414.

Milkovich, S. M., J. J. Plaut, R. J. Phillips, G. Picardi and R. Seu (2007) "MARSIS and SHARAD radar reflections within Promethei Lingula, South Polar Layered Deposits, Mars" American Geophysical Union, Fall Meeting 2007, Abstract #P11B-0545.

Mitrofanov, I. (2002) "Maps of subsurface hydrogen from the High Energy Neutron Detector, Mars Odyssey" Science 297, 78-81. doi:10.1126/science.1073616

Moorman, B. J., S. D. Robinson and M. M. Burgess (2003) "Imaging periglacial conditions with ground-penetrating radar" Permafrost and Periglacial Processes 14, 4, 319-329. doi:10.1002/ppp.463

Neal, A. (2004) "Ground - penetrating radar and its use in sedimentology: principles, problems and progress" Earth-Science Reviews 66, 261-330. doi:10.1016/j.earscirev.2004.01.004

Nieto, C. E. and R. R. Stewart (2003) "Geophysical investigations at a Mars analog site: Devon Island, Nunavut" Third Mars polar science conference.

Olhoeft, G. R. (2001) "Subsurface geophysical detection

methods to uniquely locate water on Mars" Conference on the Geophysical Detection of Subsurface Water on Mars, Houston.

Oril, G. G. and F. Ogliani (1996) "Potentiality of the ground penetrating radar for the analysis of the stratigraphy and sedimentology of Mars" Planetary and Space Science 44, 11, 1303-1315.

Osborn, G. (2006) "The Athabasca glacier, Alberta, Canada". Geological Society of America Centennia Field Guide – Rocky Mountain Section.

Paige, P. P. and J. B. Murray (2006) "Stratigraphical and morphological evidence for pingo genesis in the Cerberus plains" Icarus, 183, 46-54. doi:10.1016/j.icarus.2006.01.017

Phillips, R. J. (2007) "Results From the SHARAD Sounding Radar Experiment at Mars" American Geophysical Union, Fall Meeting 2007, Abstract #P14B-02.

Picardi, G. (1999) "The Mars advanced radar for subsurface and ionosphere sounding (MARSIS): concept and performance" International Geoscience and Remote Sensing Symposium 5, 2674-2677. doi:10.1109/IGARSS.1999.771614

Picardi, G. (2005) "Subsurface sounding in Mars Advanced Radar for Subsurface and Ionosphere Sounding (MARSIS)" Geochimica et Cosmochimica Acta 69, 10, 531.

Plaut, J. J. (2007) "An Overview of MARSIS and SHARAD Radar Sounding Observations of the Polar Deposits of Mars" American Geophysical Union, Fall Meeting 2007, Abstract #P14B-03.

Putzig, N. E., J. W. Holt, R. J. Phillips, R. Seu, D. Biccari, B. A. Campbell, L. M. Carter, A. Safaeinili and A. F. Egan (2007) "Internal Structure of the North Polar Layered Deposits on Mars From SHARAD Observations" American Geophysical Union, Fall Meeting 2007, Abstract #P11B-0544.

Reynolds, J. M. (1997) An Introduction to Applied and Environmental Geophysics, Chichester, West Sussex, Wiley.

Robinson, S. D., B. J. Moorman, A. S. Judge and S. R. Dallimore (1993) "The characterization of massive ice at Yaya Lake, Northwest Territories using radar stratigraphy techniques" Current Research, Part B, Geological Survey of Canada Paper 93-1B, 23-32.

Safaeinili, A. (2007) "Radio-Transparent Deposits in the Elysium Region of Mars as Observed by MARSIS and SHARAD Radar Sounders" Seventh International Conference on Mars, LPI Contribution No. 1353, 3206.

Seibert, N. M. and J. S. Kargel. (2001) "Small-scale Martian polygonal terrain: Implications for liquid surface water" Geophysical Research Letters 28 (5), 899-902.

Seu, R. (2007) "SHARAD sounding radar on the Mars Reconnaissance Orbiter" Journal of Geophysical Research 112, E05S05. doi:10.1029/2006JE002745

Sharp, R. P. (1973) "Mars: Fretted and chaotic terrain" Journal of geophysical research, 78, 4073-4083.

Soare, R. J., D. M. Burr, J.-M. Wan Bun Tseung and C. Peloquin (2005) "Possible pingos and periglacial landscapes in northwest Utopia Planitia, Mars" Lunar and Planetary Science Conference 36th. Abstract #1102.

Soare, R. J., D. M. Burr and J-M. Wan Bun Tseung (2005) "Possible pingos and a periglacial landscape in northwest Utopia Planitia" Icarus, 174, 373-382. doi:10.1016/j.icarus.2004.11.013

Stillman, D. E. and G. R. Olhoeft (2006) "Electromagnetic properties of Martian analog minerals at radar frequencies and Martian temperatures" Lunar and Planetary Science Conference 37th. Abstract #2002.

Tanaka, K. L., J. A. Skinner, T. M. Hare, T. Joyal and A. Wenker (2003) "Resurfacing history of the northern plains of Mars based on geologic mapping of Mars Global Surveyor data" Journal of Geophysical Research 108 (E4), 8043. doi:10.1029/2002JE001908

Theilig, E. and R. Greeley (1978) "Episodic channeling and layered terrain on Mars: Implications for ground-ice" Proceedings of the Second Colloquium on Planetary Water and Polar Processes, 151-157.

Vachon, P. W., D. Geudtner, L. Gray, K. Mattar, M. Brugman, I. Cumming and J. L. Valero. (1996) "Differential SAR interferometry measurements of Athabasca and Saskatchewan glacier flow rate" Canadian Journal of Remote Sensing 22, 3, 287-296.

Van Dam, R., W. Schlager, M. J. Dekkers and J. A. Huisman (2002) "Iron oxides as a cause of GPR reflections" Geophysics 67, 2, 536-545. doi:10.1190/1.1468614

Wan Bun Tseung, J-M. and R. J. Soare (2006) "Thermokarst and related landforms in western Utopia Planitia, Mars: Implications for near-surface excess ice" (Abstract 1414), 37th Lunar and Planetary Science Conference, March 2006.

Whalley, W. B. and F. Azizi (2003) "Rock glaciers and protalus landforms: Analogous forms and ice sources on Earth and Mars" Journal of Geophysical Research 108, E4, 8032. doi:10.1029/2002JE001864

Wohletz, K.H. and M. F. Sheridan (1983) "Martian rampart crater ejecta: experiments and analysis of melt water interaction" Icarus, 56, 1, 15-37. doi:10.1016/0019-1035(83)90125-2

Woodward, J. and M. J. Burke (2007) "Applications of ground-penetrating radar to glacial and frozen materials" Journal of Environmental and Engineering Geophysics 12, 1, 69-85.